Effect of SEPS as a Novel Compatibilizer on the Properties and Morphology of PP/PC/POE Blends

Shanshan Dai, Lin Ye

State Key Laboratory of Polymer Materials Engineering, Polymer Research Institute of Sichuan University, Chengdu 610065, China

Received 16 November 2007; accepted 28 December 2007
DOI 10.1002/app.27978
Published online 6 March 2008 in Wiley InterScience (www.interscience.wiley.com).

ABSTRACT: A novel macromolecular compatibilizer, styrene-ethylene-propylene-styrene (SEPS) with high content of styrene, was investigated for the purpose of improving the compatibility of PP (polypropylene)/PC (polycarbonate)/POE (ethylene-octene copolymer) blends. SEPS shows a remarkable compatibilizing effect since it has a particular structure with the EP-compatible aliphatic segments, which is well miscible with the nonpolar PP and olefinic elastomer POE domains, and S-chain segments which exhibit strong affinity with PC because of the similar molecular structure. Its compatibilizing effect was examined in terms of the mechanical, morphological, and thermal properties. The compatibilized PP-based blends represent remarkable improvement in impact strength and balanced tensile strength. When 5 wt % SEPS was added to PP/PC/POE blends (20 wt % POE), the impact strength of the blends was enhanced from 24 to 43 kJ/m^2 without obvious drop in the tensile strength. Their morphologies show a decreasing and much more homogeneous size of dispersed PC and POE particles through addition of SEPS, and the fracture surface morphologies change from irregular mosaic to the mix of mosaic and striation, and finally the regularly distant striation. The special morphology structure that resulted from the effect of the compatibilizer could be a key for enhancement of toughness and balanced rigidity of the blends. © 2008 Wiley Periodicals, Inc. J Appl Polym Sci 108: 3531–3541, 2008

Key words: polypropylene; polycarbonates; compatibilization; toughness; blends

INTRODUCTION

Polypropylene (PP) is one of the largely produced and consumed polyolefins in the plastic industry. It is known to exhibit low impact strength, which greatly limits its engineering structural applications. A main goal in the development of PP-based blends is practically always to achieve processable materials of high impact resistance combined with sufficient stiffness.[1–21] Rubber modification has been proved to be effective in toughening PP even at low temperatures (i.e., -20°C),[1–3] and extensive research has been published on the blends of PP with ethylene-propylene rubber, ethylene-propylene-diene copolymer, and styrene-ethylene-butylene-styrene triblock copolymer. Nowadays, interests have centered on the use of ethylene-octene copolymer (POE) which is the most potential kind of elastomer as toughness modifier.[4,5] Unfortunately, the accompanying penalty from rubber toughening usually represents a noticeable reduction in modulus and scratch/mar resistance of materials, which cannot be completely solved by further addition of inorganic fillers,[6–11] although it is supposed to increase the modulus of PP. A delicate balance among modulus, yield/brittle stress, yield/brittle strain, and toughness has to be reached to achieve the system with all improved toughness, strength, modulus, and acceptable scratch resistance. Consequently, based on a new concept ''rigid–rigid polymer toughening,'' it is possible to improve toughness and maintain modulus of PP by blending PP with a rigid engineering polymer, such as polyamide.[12–16]

Recently, polycarbonate (PC) as an engineering plastic has attracted the attention of technologists because of the advantages that it provides over conventional materials, namely, the excellent combination properties of stiffness, strength, toughness, ductility, impact resistance, and transparency.[17] The main purpose of this work is to counteract the effect of POE by selectively reinforcing the PP matrix with PC particles. However, PP and PC or POE and PC are immiscible with each other attributing to evident differences in their polarity and solubility parameters.[18–21] Thus, much investigation has initially been focused on compatibilizing these polymer pairs, and then establishing the relationship between the morphology and mechanical behaviors of such polymer

Correspondence to: L. Ye (yelinwh@126.com).
Contract grant sponsor: National Basic Research Program of China; contract grant number: 2005CB623800.
Contract grant sponsor: Program for Changjiang Scholars and Innovative Research Team in University; contract grant number: IRT0449.

Journal of Applied Polymer Science, Vol. 108, 3531–3541 (2008)

blends to exploit the advantages of PC in PP matrix. Macromolecular compatibilizer improves two important factors affecting the properties of polymer blends: the morphology of the dispersed phase and the interfacial adhesion between the dispersed phase and the matrix,[22,23] and this work concentrated on the study of the compatibilizing effect of the novel compatibilizer-styrene-ethylene-propylene-styrene (SEPS) on PP/PC blend.

EXPERIMENTAL

Materials

The materials used in this research included the following: (1) PP, T30S, was produced by Dushanzi Petrochemical (Kelamayi, China), with melt flow index (MFI) 2.5–3.5 g/10 min (230°C, 2.16 kg); (2) PC, L1250Y, was supplied by Teijin (Matsuyama, Japan), with MFI 6.7 g/10 min (300°C, 1.2 kg); (3) POE, Engage 8150, was purchased from Dupont-Dow Chemicals (Washington, DC), with 39% octene; (4) SEPS, Septon 2104, was produced by Kuraray (Okayama, Japan), with 65 wt % of styrene. (5) The antioxidant tetrakis-[methylene-β-(3,5-di-*tert*-butyl-4-hydroxyphenyl)-propionate] methane (1010) was supplied by Ciba-Geigy (Basel, Switzerland).

Sample preparation

PP-based blends with the compatibilizers were prepared in a TSSJ-25/03, corotating, twin-screw extruder at a rotational speed of 90 rpm. The temperature of the barrel was in the range of 220–270°C. Corresponding extrudates were hauled into a quenching water trough prior to being palletized. Dried blends were molded to form impact and tensile specimens by using a K-TEC40 injection molding machine. The barrel temperature profile was 260°C (hopper)–280°C (nozzle), and the mold temperature was maintained at 50°C.

Characterizations

The tensile strength of the samples was measured with 4302 material testing machine from Instron (USA) according to ISO527/1-1993 (E). The test speed was 50 mm/min, and the sample length between bench marks was 50 ± 0.5 mm. The notched charpy impact strength of the samples was measured with ZBC-4B impact testing machine from Xinsansi (Shenzhen of China) according to ISO179-1993 (E).

The dynamic mechanical analysis was performed with DMA Q800 (USA) by using clamp single cantilever mode with a frequency of 1 Hz. The temperature scanning ranged from −80 to 160°C with a heating rate of 3°C/min.

The nonisothermal crystallization was performed with a NETZSCHDSC 204 (Germany). Samples of 5–10 mg were heated quickly from ambient temperature to 280°C under nitrogen atmosphere, and kept for 5 min before crystallization to eliminate the effect of the previous thermal history, and then cooled to 50°C with a rate of 10°C/min.

A wide-angle X-ray diffraction measurement was carried out with a Philip X'Pert Graphic & Identify instrument (The Netherlands) at room temperature to determine crystal parameters of samples. The materials were taken from the skin and core layer of the samples. The Cu Kα irradiation source was operated with a step size of 0.02° from 2θ = 10°–40°. The *d*-spacing is calculated by substituting the scattering angles of the peak into the Bragg's equation[24] as follows:

$$d = \frac{\lambda}{2 \sin \theta} \quad (1)$$

where θ is the X-ray diffraction angle and wave length λ = 0.153 nm.

Cryogenically fractured in liquid nitrogen, and etched with cyclohexane to dissolve the POE and SEPS phase, the fracture surfaces of the blends were sputter-coated with a thin gold layer to make samples electric conductive, avoiding the charge accumulated, and then observed by a JEOL JSM-5900LV scanning electron microscopy (SEM) instrument with an acceleration voltage of 20 kV. To study the toughening mechanism, the impact-fractured surface of the blends was directly observed under the same condition without etching.

RESULTS AND DISCUSSION

Mechanical properties of PP-based blends

In general, the mechanical properties of polymer can be roughly classified into two categories: strength and toughness. Tensile strength and modulus can be considered as the material strength, while tensile toughness and impact strength are the material toughness.[25] The tensile and notched charpy impact strength of PP/PC/POE blends as a function of the content of the compatibilizer (SEPS) is summarized in Figure 1. Modification of a polymeric material seldom results in the improvement of both strength and toughness simultaneously.[26] As expected, with the increase of the content of POE from 10 to 20 wt %, the impact strength of the PP-based blends increased significantly and they became more ductile. In the meantime, the tensile strength of the samples was impaired substantially. Compared with the ternary blend (PP/PC/POE), the impact strength of PP/PC/POE/Compatibilizer systems is significantly improved, and further increasing SEPS loading results in more increment of impact strength

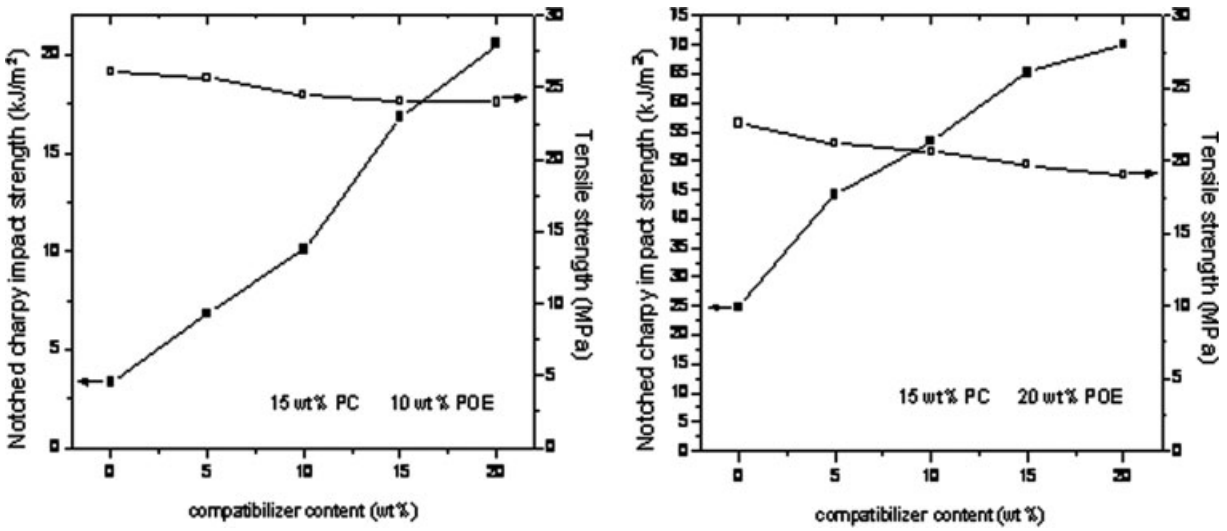

Figure 1 The notched charpy impact strength and tensile strength of PP/PC/POE/Compatibilizer blends.

although the extent reduces gradually. Additionally, all the samples retained relatively high values of tensile strength. The improvement in impact strength of the blends led by addition of compatibilizer was more pronounced at high content of POE. When 5 wt % SEPS was added to PP/PC/POE blends (20 wt % POE), the impact strength of the blends was enhanced from 24 to 43 kJ/m^2 without obvious drop in the tensile strength (about 1 MPa).

The mechanical behavior of a blend is determined by the contribution of each component, as well as by the blend morphology and the interfacial adhesion. POE may cause deformation or form microvoid that can absorb large amount of energy during being impacted and improve toughness of these blends.[27] The further toughness improvement of the compatibilized PP-based blends indicates that compatibilizing effect of SEPS is remarkable because of its particular structure with EP-compatible aliphatic segments that can mix well with the nonpolar PP and olefinic rubber POE domains and S-chain segments, which exhibit strong affinity with PC because of the similar molecular structure. The use of SEPS to strengthen the interface of polymeric components which lack strong interactions has emerged to decrease the interfacial tension and increase the chain entanglement within the interphase. The linkage between incompatible components is established, and the grossly immiscible PP/PC/POE system becomes miscible. Therefore, the toughness and stiffness of these blends are in good balance.

Based on the conclusion mentioned earlier and the mechanical properties of PP/PC/Compatibilizer blends as shown in Table I, it can be seen that although it is a kind of SBS block polymer, SEPS with 60 wt % styrene selected in this work provides the compatibilizer with relatively high stiffness and weak toughness. When 25 wt % SEPS is added into PP/PC blends, the impact strength of the blends only rise to 4.97 kJ/m^2, and the enhancement of elongation at break which is sensitive to the load transfer between phase is also slight. It can be demonstrated that SEPS cannot toughen PP as elastomer but effectively compatibilize PP/PC/POE ternary system, and then improve toughness and maintain modulus of PP-based blends.

Dynamic mechanical properties of PP-based blends

Dynamic mechanical analysis (DMA) is a very important tool in ascertaining the performance of a material under stress and temperature. Figure 2 is a composite plot of temperature dependence of the storage modulus, loss modulus, and loss tan δ of the component

TABLE I
The Mechanical Properties of PP/PC/Compatibilizer Blends

Sample	Notched charpy impact strength (kJ/m^2)	Tensile zstrength (MPa)	Tensile modulus (MPa)	Elongation at break (%)
PP/PC/Compatibilizer: 85/15/0	2.34	33.07	930.2	97.4
PP/PC/Compatibilizer: 80/15/5	2.53	32.38	856.6	104.0
PP/PC/Compatibilizer: 70/15/15	3.98	30.84	778.0	157.4
PP/PC/Compatibilizer: 60/15/25	4.97	30.60	711.1	147.1

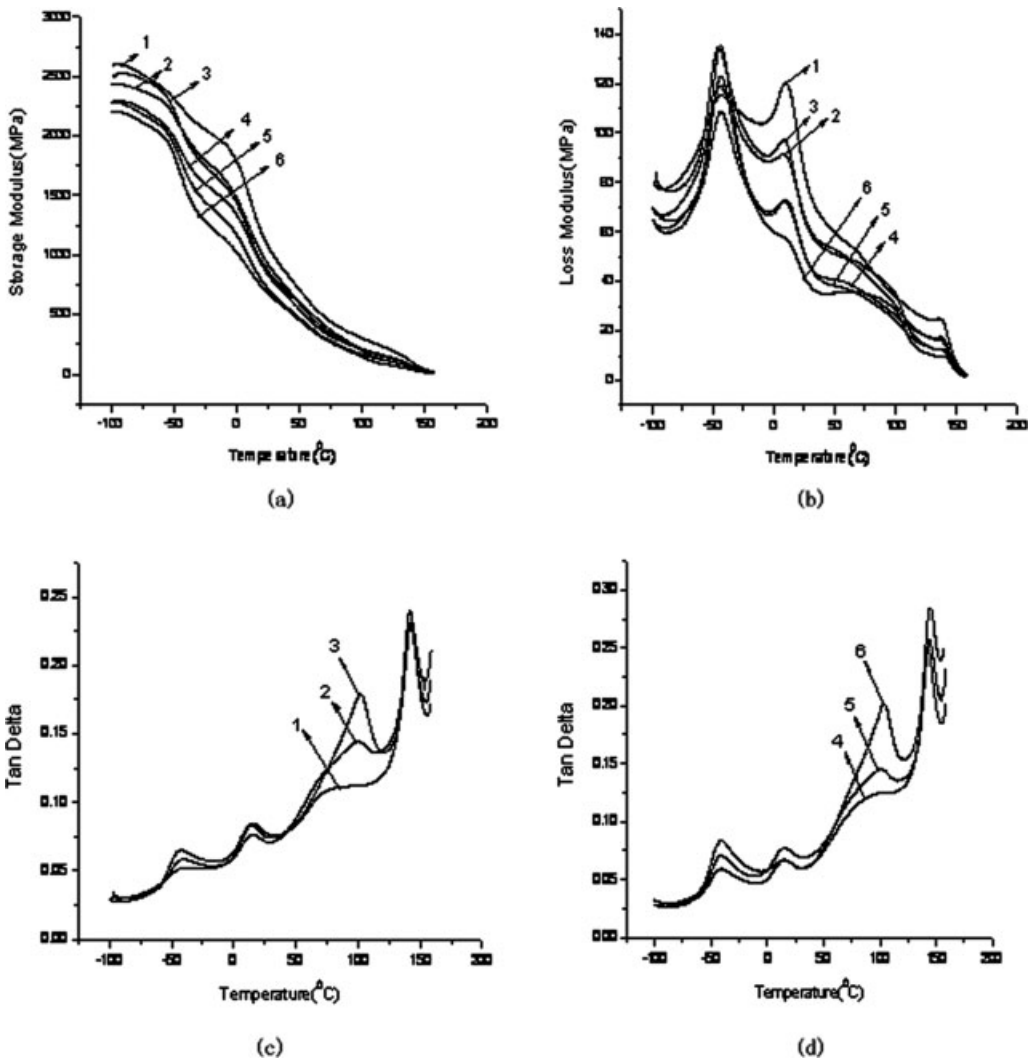

Figure 2 DMA curves of PP blends (1) PP/PC/POE/Compatibilizer (75/15/10/0); (2) PP/PC/POE/Compatibilizer (65/15/10/10); (3) PP/PC/POE/Compatibilizer (55/15/10/20); (4) PP/PC/POE/Compatibilizer (65/15/20/0); (5) PP/PC/POE/Compatibilizer (55/15/20/10); (6) PP/PC/POE/Compatibilizer (45/15/20/20).

polymers in the selected blends. The storage modulus is directly related to the elastic response of the tested material, and tan δ is intimately associated with the chain relaxation that takes place.[28] All the storage modulus and temperature curves, as shown in Figure 2(a), experience a gradual decline in storage modulus with increase in temperature from −100 to 160°C. The addition of POE leads to a reduction in storage modulus obviously, and when more POE was added, there was more reduction in the modulus. The loss modulus and loss tan δ reveal more clearly the corresponding transition temperatures and the width of transition zones [Fig. 2(b–d)]. In PP/PC/POE ternary system, the glass transition of POE occurs at −50 to −20°C with a peak at about −40°C. There exists a β-transition of PP at −10 to 35°C with a peak at about 14°C and a α-relaxation peak around 90°C. The glass transition peak of PC is noted at around 145°C in the heating cycle. These well-separated transitions are indicative of immiscibility of the component polymers. Temperature dependence of the storage modulus, loss modulus, and loss tan δ of neat compatibilizer is shown in Figure 3 for comparison. The most interesting observation in Figure 2 is the appearance of a new transition peak around 100°C by addition of SEPS in PP/PC/POE blends. The peak temperature of the new transition is a little lower than that of neat SEPS (107°C). When more SEPS was added, broader and stronger transition is noted in this region and the transition shifts to higher temperature in the meantime, in other words, more close to the transition temperature of SEPS.

Generally, glass transition shifts in the blends can be explained based on the physical interactions between the components.[29] Compared with small molecules, it is more difficult for SEPS as a macromolecular compatibilizer to mix with other components in the molecular level. The observed shift in

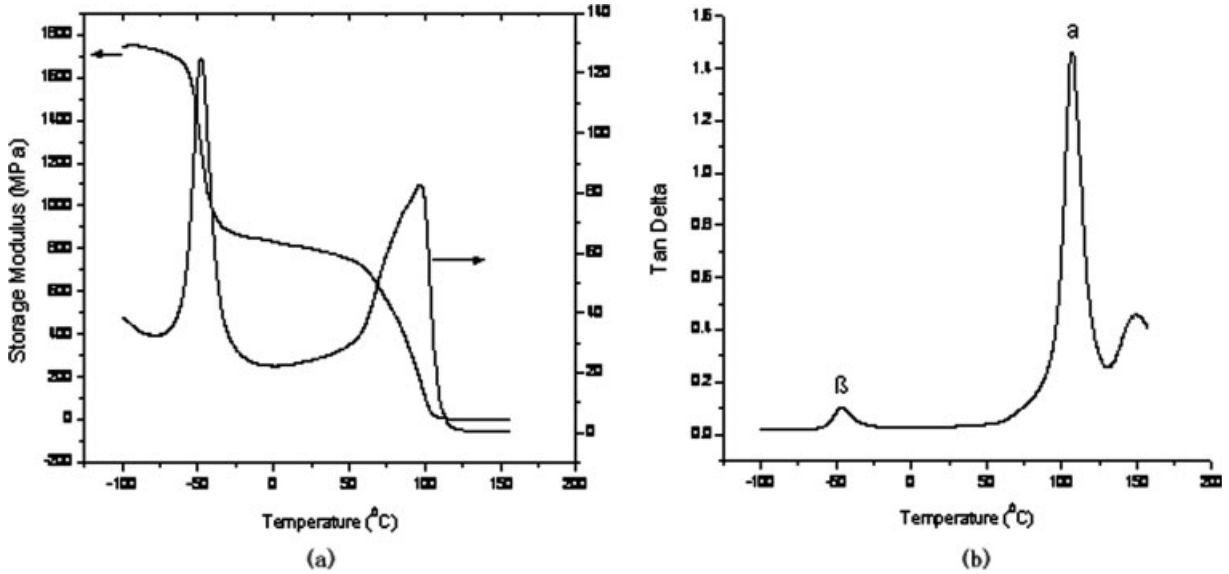

Figure 3 DMA curves of compatibilizer.

glass transition values of PP, POE, and PC in these compatibilized blends (Table II) is not expected because such variations are normally not observed in partially or fully miscible blends, but the data of DMA clearly shows that by the addition of SEPS a new interphase domain forms, in which SEPS and the other polymer components of the blends are miscible with each other, and tends to decrease the interfacial tension and improve the compatibility of PP/POE/PC.

Crystallization properties of PP-based blends

Nonisothermal differential scanning calorimetry analysis of PP-based blends

Nonisothermal crystallization is significant because it is very close to practical process.[30] The major differences in thermal behavior for different PP-based blends occurred during the differential scanning calorimetry (DSC) cooling scan period, as shown in Figure 4 and Table III. PP is highly crystalline polymer with typical thermal behavior that can crystallize rapidly even under quenched conditions. Apparently, the chain structure and phase morphologies of blends, which will be investigated by SEM experiments hereinafter, are quite complex, which inevitably imply there are various reasons affecting crystallization. In Figure 4, each PP-based blend exhibit only a single crystallization peak, which is attributed to the crystallization of PP. In PP/PC/POE ternary blends, the crystallization peaks of PP (T_{peak}) are affected by the presence of PC and POE, respectively. The solidification of PC particles dispersing in the PP melt easily results in heterogeneous nucleation, which significantly increases the peak temperature (T_{peak}) of the crystallization exotherm of PP, on the other hand, the encapsulation of the dispersing PC by SEPS reduces the degree of the direct interfacial contact between PP and PC particles, and this compatibilizing effect of SEPS will improve the interfacial adhesion of PP/PC/POE blends but reduce the heterogeneous nucleation at the same time. The latter one is more obvious during the crystallization process of these PP-based blends, and the crystallization peaks of PP shift to lower temperatures with the addition of SEPS. More SEPS leads to further decrease in crystallization temperature. The compatibilized system also presents the broader crystalline half-peak width and lower crystalline enthalpy,

TABLE II
DMA Data of PP-Based Blends and Compatibilizer

Sample	T_g (PC)	T_g (Compatibilizer)	T_g (PP)	T_g (POE)
PP/PC/POE/Compatibilizer (75/15/10/0)	141.72	/	15.10	−42.10
PP/PC/POE/Compatibilizer (75/15/10/10)	141.72	100.15	13.96	−41.72
PP/PC/POE/Compatibilizer (75/15/10/20)	142.87	101.68	13.20	−41.34
PP/PC/POE/Compatibilizer (75/15/20/0)	142.48	/	15.49	−41.72
PP/PC/POE/Compatibilizer (75/15/20/10)	144.01	100.91	15.87	−41.34
PP/PC/POE/Compatibilizer (75/15/20/20)	144.91	103.98	16.32	−41.07
Compatibilizer	/	107.09	/	/

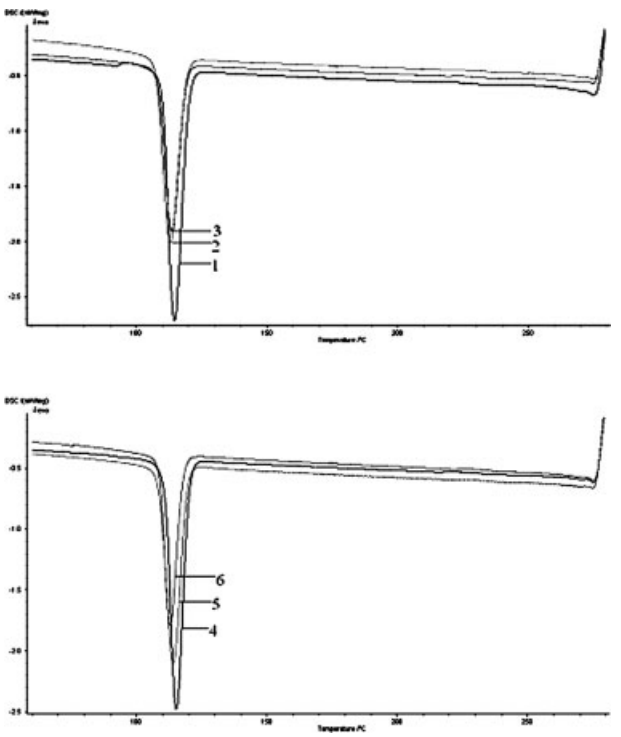

Figure 4 DSC curves of PP blends (1) PP/PC/POE/Compatibilizer (75/15/10/0); (2) PP/PC/POE/Compatibilizer (65/15/10/10); (3) PP/PC/POE/Compatibilizer (55/15/10/20)blends; (4) PP/PC/POE/Compatibilizer (65/15/20/0); (5) PP/PC/POE/Compatibilizer (55/15/20/10); (6) PP/PC/POE/Compatibilizer (45/15/20/20).

which indicate the decreasing of the crystalline growth rate and crystallinity of the PP blends.

X-ray diffraction of PP-based blends

Figure 5 shows the X-ray diffraction (XRD) scans of PP and PP/PC/POE blends with increasing content of the compatibilizer. The detailed analysis of neat PP is given in Table IV. The samples were taken from skin or core layer of the injection-molded specimens. The typical crystalline form for isotactic PP is α-form with a characteristic diffraction peak at about 18.6° corresponding to the 130 plane diffraction as observed. Core layer of PP displays a prominent increase in the density at lower 2θ values when compared with skin layer of PP. This clearly reflects that distribution of shearing force during injection is a very important factor affecting crystallization of polymer. It can also be observed that all the PP-based blends are amorphous, which would be associated with the molecular mixing. Thus a strong influence of blending PP with PC/POE on the behavior of conversion of material from a crystalline to the amorphous state is clearly seen in Figure 5. When the compatibilizer-SEPS was added in the blends, the characteristic peaks of skin and core layer slightly decreased and shrinked, indicating that the extent of amorphous region increased slightly.

Scanning electron microscopy analysis of PP-based blends

Morphologies of PP-based blends

Mechanical strength is related to the morphology, domain size, and size homogeneity of the polyblends, and it is believed that interaction between two phases is one of the key factors deciding the degree of dispersion.[31] Generally speaking, an effective compatibilizer endows polyblends with finer phase domain size, greater interfacial contact area, and higher interfacial adhesion. When the rigid PC particles are added in PP/POE blends, and depending on the location of PC, three types of microstructures may form: ''separate'' dispersion structure, where the PC particles reside in the matrix and not coated with POE; encapsulation or core-shell structure, where PC particles partition preferentially in the dispersed phase POE; and mixture of the former two. A separated microstructure, wherein the rigid particles partitions favorably in the PP matrix, without affecting the elastomer phase, is desirable for optimum reinforcement

TABLE III
Effect of Compatibilizers on the Crystallization Parameters of PP-Based Blends

Sample	T_{peak} (°C)	T_{onset} (°C)	T_{end} (°C)	ΔW (50%, °C)	X_c (%)	ΔH (mW/mg)
1	114.7	110.1	120.2	5.9	43.07	2.291
2	113.1	107.7	119.3	6.9	36.74	1.713
3	113.6	108.6	119.1	6.3	29.85	1.523
4	115.4	111.2	120.4	5.4	35.17	2.059
5	114.2	108.9	119.5	6.2	32.26	1.633
6	113.0	109.0	118.0	5.3	24.08	1.416

1: PP/PC/POE/Compatibilizer (75/15/10/0); 2: PP/PC/POE/Compatibilizer (65/15/10/10); 3:PP/PC/POE/Compatibilizer (55/15/10/20); 4: PP/PC/POE/Compatibilizer (65/15/20/0); 5: PP/PC/POE/Compatibilizer (55/15/20/10); 6: PP/PC/POE/Compatibilizer (45/15/20/20).

T_{onset}, the onset crystallization temperature; T_{peak}, the crystallization peak temperature; T_{end}, the end crystallization temperature; X_c, the crystallinity; ΔH, the crystalline enthalpy; ΔW, the crystalline half-peak width.

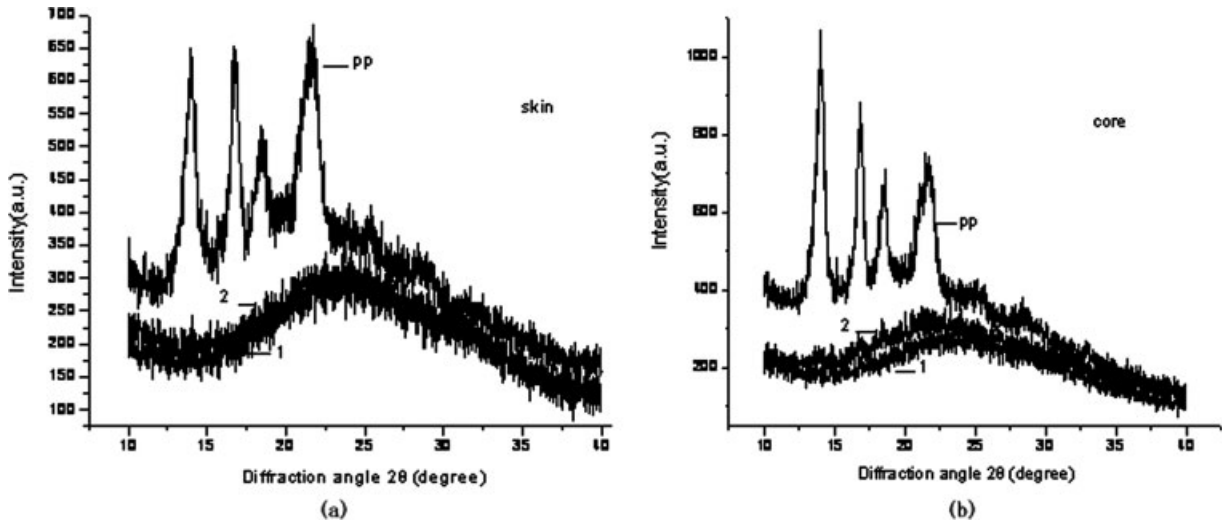

Figure 5 XRD patterns of PP and PP-based blends.

of blends. As shown in Figure 6, SEM images of etched skin layer of PP-based blends clearly reveals the morphologies of the uncompatibilized and compatibilized blending systems at the magnification of 5000×. In the skin layer of the blends, most PC particles (bright particles) localize exclusively in the PP matrix phase and formed the desired separated microstructure without affecting the POE phase, because PC particles will be effectively forced out from high viscosity of POE and eventually agglomerate together in PP matrix or SEPS domains under the shear force. The dark holes and slots formed by shear stress during injection molding represent the etched POE particles and SEPS phase. PC particles are nonuniformly distributed over the skin layer of the blends, and smooth interface between PP and PC is observed for the blends with 10 and 20 wt % POE, as shown in Figure 6(a,d). It reveals a poor adhesion between phases in the absence of the compatibilizer agent (SEPS), as demonstrated by the fracture developing along the interface. Moreover, very small amount of the dark holes and slots can be observed for the blends with low content of POE, indicating that there appears little POE in the skin layer of the blends in this case. The addition of SEPS leads to a decreasing and much more homogeneous size of the dispersed PC particles in the skin layer of the blends, and large amount of dark holes and slots representing the POE and SEPS phase can be observed clearly.

As shown in Figure 7(a,d), in the core layer, the ternary PP/PC/POE blends exhibit very big spherical-shaped domains which may be formed by PC. The residue holes in polyblends are formed by the etched POE phase. It can be easily concluded that PC and POE phase dispersed in the PP matrix, respectively, forming the ''separate'' dispersion structure as in the skin layer. Smooth and clean interface between PP and PC results in the great interfacial tension and weak adhesion between PP and PC. As expected, the addition of SEPS results in decreasing and much more homogeneous size of the dispersed PC phase, which change to rod-like in shape in the mean time and the extent is enhanced with the increase of the content of SEPS. Some of the PC phase are encapsulated by SEPS as shown in Figure 7(c,f). On the other hand, the addition of SEPS not only leads to the much finer phase domain size, but also makes the boundary between PP and PC phase dimmer, indicating the decrease of interfacial tension and enhancement of adhesion between PP and PC, which is beneficial to the improvement of

TABLE IV
XRD Analysis of PP

d-Spacing (nm)	Angle (2θ)	Relative intensity (%)	Tip width (2θ)
Skin layer			
6.32	14.00	87.62	0.32
5.63	15.72	17.76	0.12
5.31	16.68	84.82	0.20
5.25	16.88	87.00	0.16
4.79	18.52	63.43	0.56
4.10	21.64	100	0.96
3.51	25.35	32.56	0.48
3.14	28.73	19.11	1.28
Core layer			
6.31	14.01	100	0.44
5.26	16.85	76.22	0.24
4.83	18.36	45.59	0.28
4.78	18.56	52.16	0.16
4.23	21.00	50.40	0.24
4.10	21.66	64.69	0.56
3.50	25.41	18.80	0.96
3.13	28.52	15.54	0.32
2.72	32.93	7.16	0.48

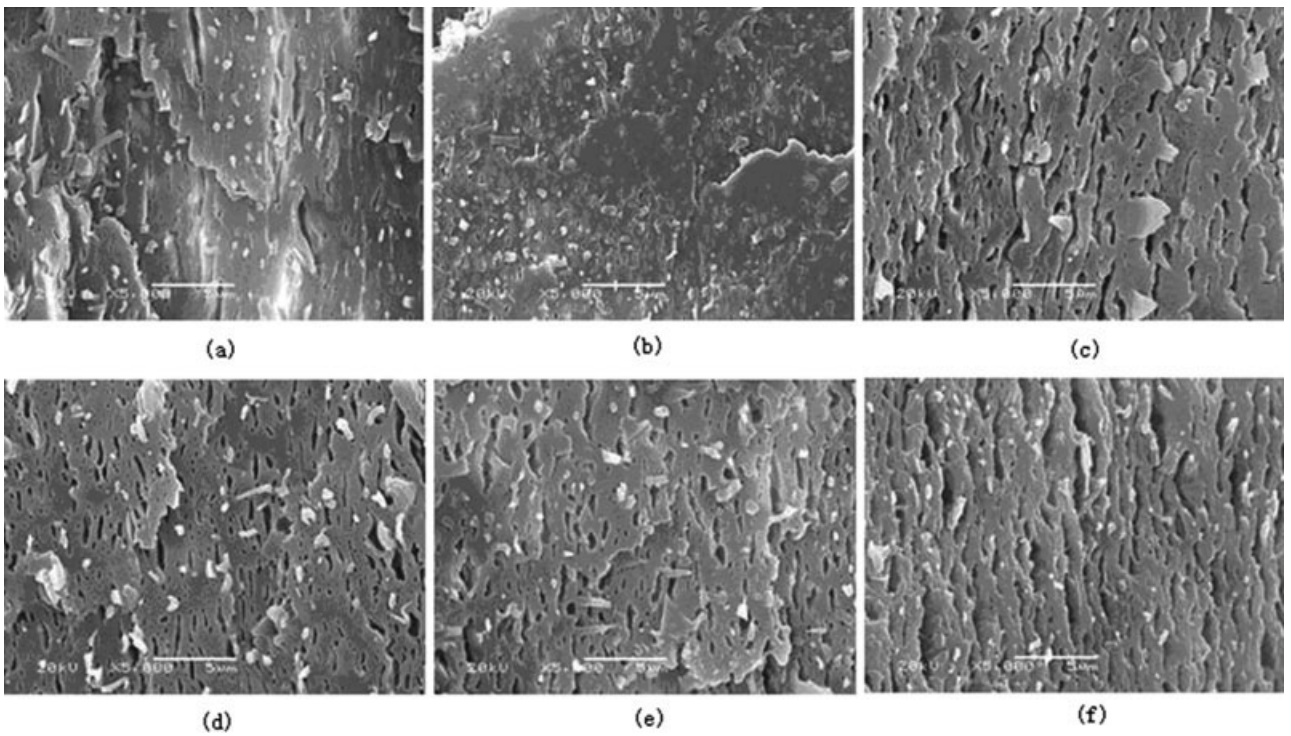

Figure 6 SEM images of etched skin layer of PP blends (a) PP/PC/POE/Compatibilizer (75/15/10/0); (b) PP/PC/POE/Compatibilizer (65/15/10/10); (c) PP/PC/POE/Compatibilizer (55/15/10/20); (d) PP/PC/POE/Compatibilizer (65/15/20/0); (e) PP/PC/POE/Compatibilizer (55/15/20/10); (f) PP/PC/POE/Compatibilizer (45/15/20/20).

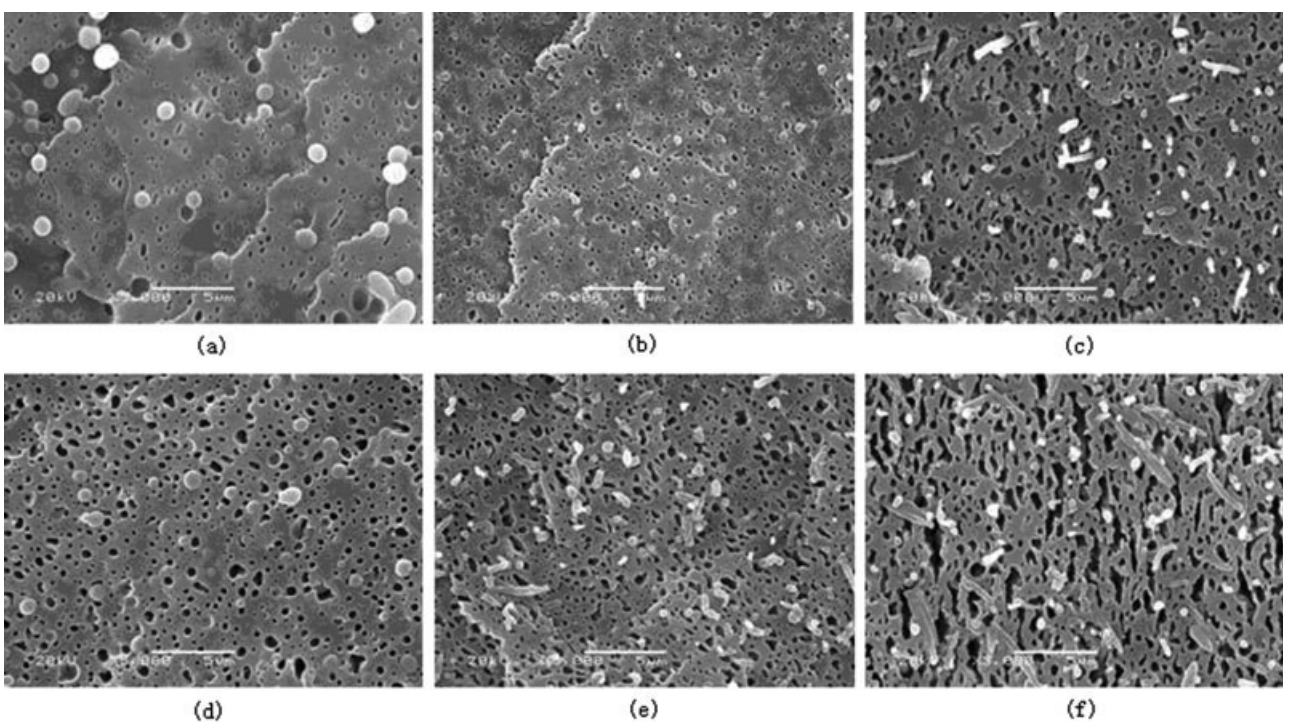

Figure 7 SEM images of etched core layer of PP blends (a) PP/PC/POE/Compatibilizer (75/15/10/0); (b) PP/PC/POE/Compatibilizer (65/15/10/10); (c) PP/PC/POE/Compatibilizer (55/15/10/20); (d) PP/PC/POE/Compatibilizer (65/15/20/0); (e) PP/PC/POE/Compatibilizer (55/15/20/10); (f) PP/PC/POE/Compatibilizer (45/15/20/20).

the mechanical properties of the blends. With 20 wt % POE and 20% SEPS loading, the morphologies of the blend are coral-like in the perpendicular plane, close to the co-continuous phase morphology. It is reasonable to believe that this kind of phase structure of the PP-based blends explains, to some extent, why the material can keep a good balanced rigidity and toughness.

Toughening mechanism of PP-based blends

Toughening mechanism in rubber-modified single-phase polymers has been well established.[32–35] According to the framework of Wu's theory,[36–38] for polymer/elastomer binary blend, a sharp brittle–ductile transition occurs at a critical matrix-ligament thickness or the critical surface-to-surface interparticle distance τ_c, described by:[22]

$$\tau_c = d_c\left[\left(\pi/6\phi_r\right)^{1/3} - 1\right] \quad (2)$$

where d_c is the critical elastomer particle diameter, and ϕ_r is the volume fraction of the elastomer. If τ (average value) $< \tau_c$, the continuum percolation of stress volume around elastomer particles would occur. The matrix yielding would propagate through the entire matrix, and then the blend would be tough. On the contrary, if $\tau > \tau_c$, the matrix yielding could not propagate, and the blend failed in a brittle manner. Further insight into the results of phase morphology discussed earlier, in PP/PC/POE/Compatibilizer blends, dispersed POE particle size is obviously decreased and effectively reduces the interparticle distance. Besides, the stress field around PC particles can interfere or overlap with those around POE particles when POE particles are close to rigid particles after compatibilizing. In this case, the stress fields around PC particles seem to serve as a bridge between two neighboring elastomer particles. Therefore, the synergic effect of these two factors is believed to result in the observed increase of impact strength in the compatibilized blends.

The morphology of the impact fracture surfaces of the skin and core layer of PP-based blends, as shown in Figures 8 and 9, provides a better understanding of the toughening mechanism. The cavitation of isolated elastomer particles and SEPS interlayers represents the main mechanisms of damage and volume dilatation for polymer blends. Deformation damage is essentially controlled by elastomer cavitation and interfacial debonding. The dissipation of impact energy in the blends is probably because of the following factors: first, the isolated elastomer particles play a significant role in either arresting the cracks or at least reducing their propagation rate; second, the high adhesion of the interfacial layer avoids early decohesion between PP and PC, and is later

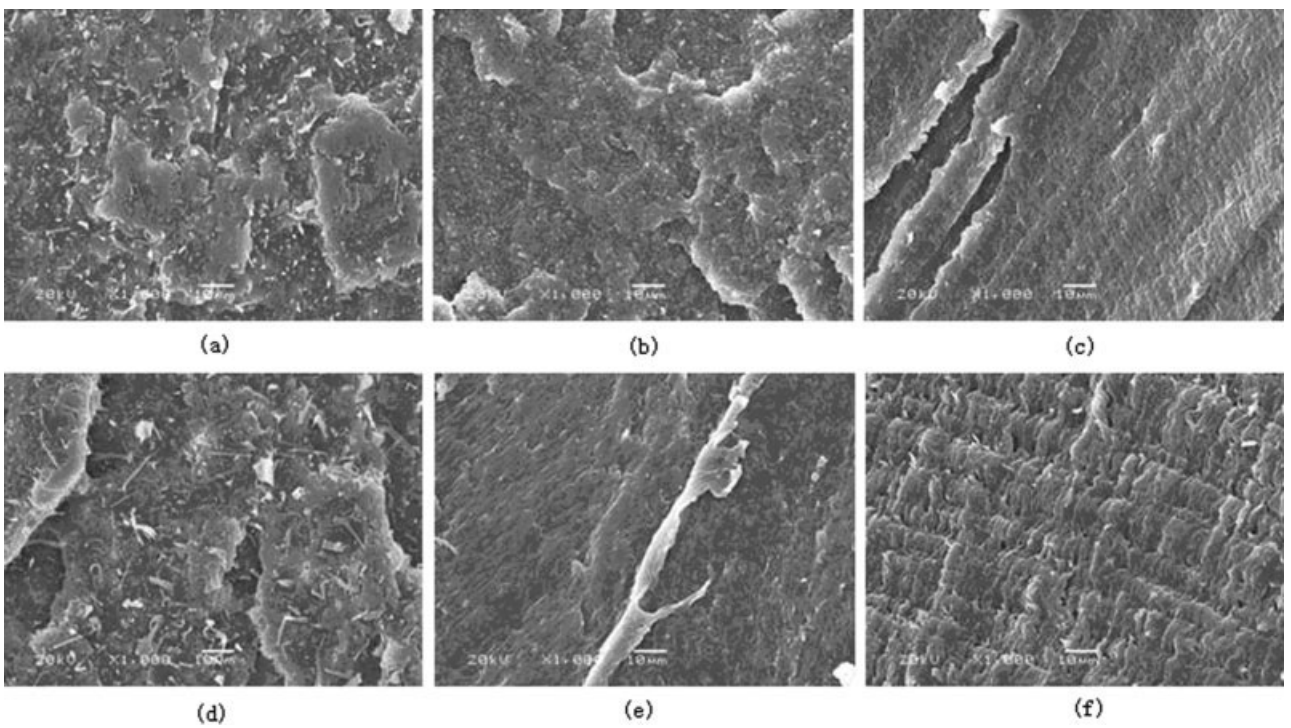

Figure 8 SEM images of impact fracturing skin layer of PP blends (a) PP/PC/POE/Compatibilizer (75/15/10/0); (b) PP/PC/POE/Compatibilizer (65/15/10/10); (c) PP/PC/POE/Compatibilizer (55/15/10/20); (d) PP/PC/POE/Compatibilizer (65/15/20/0); (e) PP/PC/POE/Compatibilizer (55/15/20/10); (f) PP/PC/POE/Compatibilizer (45/15/20/20).

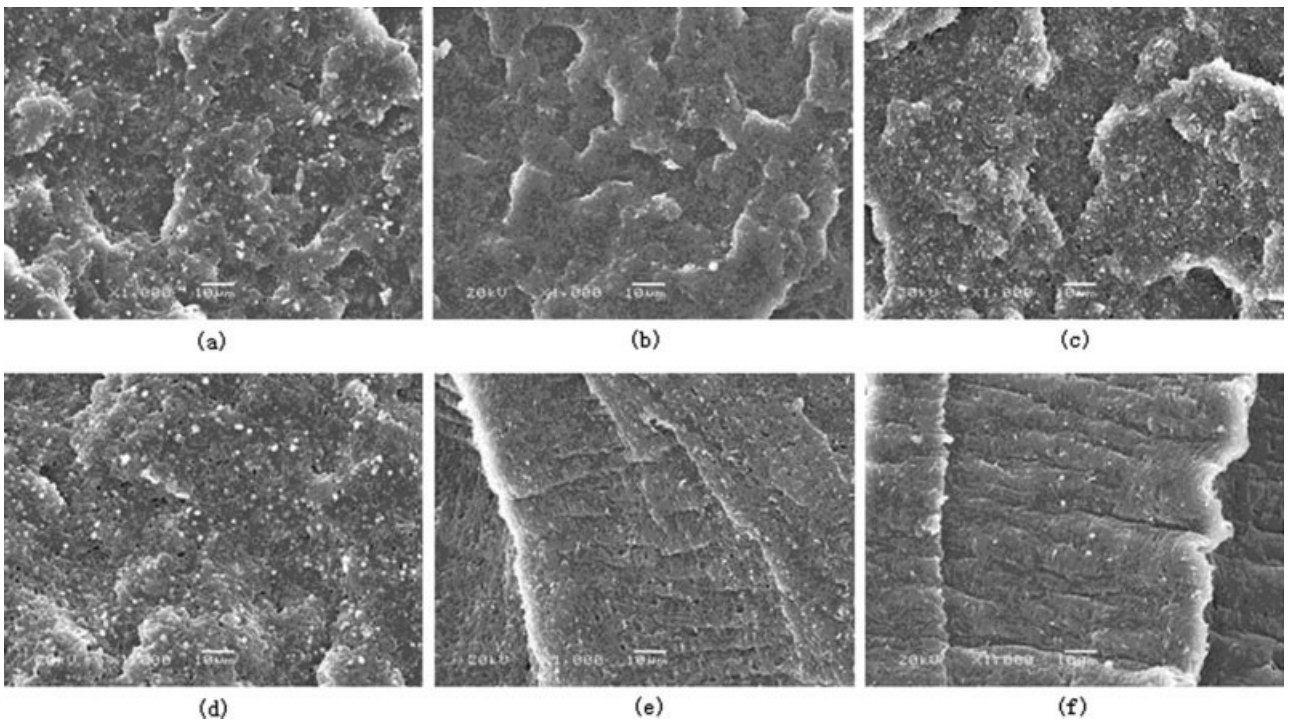

Figure 9 SEM images of impact fracturing core layer of PP blends (a) PP/PC/POE/Compatibilizer (75/15/10/0); (b) PP/PC/POE/Compatibilizer (65/15/10/10); (c) PP/PC/POE/Compatibilizer (55/15/10/20); (d) PP/PC/POE/Compatibilizer (65/15/20/0); (e) PP/PC/POE/Compatibilizer (55/15/20/10); (f) PP/PC/POE/Compatibilizer (45/15/20/20).

capable of cavitation; third, rod-like geometry of the particles improves somehow the impact resistance due to its favorable orientation perpendicular to the crack propagation direction. As for the good modulus and yield strength, it is due to the adequately combined effect of rigid PC and flexible POE, the orientation of the rod-like PC particles playing positive role in this balance.

Before compatibilizing, the crack propagated easily across the section and left smooth fracture surfaces and much sharp split as shown in Figures 8(a,d) and 9(a,d), namely, the material presents brittle fracture (mosaic), indicating the comparatively low interfacial adhesion which is markedly destroyed when the specimen is subjected to being impacted. For blending with a small amount of SEPS, enhanced interlayer and appearance of rod-like dispersed PC phase result in the decreasing of sharp split and the increasing of roughness. The fracture surfaces change from irregular mosaic to the mix of mosaic and striation. Further increase of the content of SEPS, the character of tough fracture presents much more obvious, and the fracture surface is fully covered with the regularly distant striation as shown in Figures 8(f) and 9(f), in agreement with the results of the mechanical properties.

CONCLUSIONS

The compatibilizing effect of SEPS on PP/PC/POE blend was studied by the measurement of mechanical properties, DMA, DSC, XRD, and SEM analysis. SEPS displays obvious compatibilizing effect, and the blend PP/PC/POE/Compatibilizer represents remarkably improved mechanical properties with balanced toughness and rigidity because of the particular miscible structure of SEPS with PP, POE, and PC. The data of DMA clearly show that addition of SEPS tends to form the interphase domains, in which there mainly contains SEPS and the polymer components are miscible to each other. Compatibilizing effect of SEPS will improve the interfacial adhesion of PP/PC/POE blends, but reduces the degree of the direct interfacial contact between PP and PC particles in the meantime. The crystallization peaks of PP blends shift to a lower temperature, and crystalline growth rate and crystallinity also decreased with the addition of SEPS because of its negative effect on the heterogeneous nucleation of PC in PP matrix. The blending morphologies show much dimmer boundary between the dispersing phase and the matrix, from spherical to rod-like phase of the dispersed PC particles and much more decreased size of PC and POE particles by the addition of SEPS. The fracture surface morphologies change from irregular mosaic to the mix of mosaic and striation, and finally the regularly distant striation. The high toughness is controlled by the intrinsic resistance of the PC particles, rod-like geometry of PC particles, adhesion of the interfacial layers, and the profuse cavitation in the isolated POE particles.

References

1. Yang, H.; Zhang, X. Q.; Qu, C. Polymer 2007, 48, 860.
2. Borggreve, R. J. M.; Gaymans, R. J.; Schuijer, J. Polymer 1987, 28, 1489.
3. Srinivasan, K. R.; Gupta, A. K. J Appl Polym Sci 1994, 53, 1.
4. Yang, J. H.; Zhang, Y.; Zhang, Y. X. Polymer 2003, 44, 5047.
5. Bai, S. L.; Wang, G. T.; Hiver, J. M.; G'Sell, C. Polymer 2004, 45, 3063.
6. Sahnoune, F.; Lopez Cuesta, J. M.; Crespy, A. Polym Eng Sci 2003, 43, 647.
7. Sung, Y. T.; Han, M. S.; Song, H. K.; Jung, J. W.; Lee, H. S.; Kum, C. K. Polymer 2006, 47, 4434.
8. Chang, S. Q.; Xie, T. X.; Yang, G. S. J Appl Polym Sci 2006, 102, 5184.
9. Fisher, I.; Siegmann, A.; Narkis, M. Polym Compos 2002, 23, 34.
10. Zhang, L.; Li, C. Z.; Huang, R. J Polym Sci Part B: Polym Phys 2005, 43, 1113.
11. Yang, H.; Zhang, Q.; Guo, M.; Wang, C.; Du, R. N.; Fu, Q. Polymer 2006, 47, 2106.
12. Wei, G. X.; Sue, H. J.; Chu, J.; Huang, C.; Gong, K. Polymer 2000, 41, 2947.
13. Wilkinson, A. N.; Clemens, M. L.; Harding, V. M. Polymer 2004, 45, 5239.
14. Liu, X. H.; Wu, Q. J.; Berglund, L. A.; Fan, J. Q.; Qi, Z. N. Polymer 2001, 42, 8235.
15. Jannerfeldt, G.; Boogh, L.; Manson, J. A. E. J Polym Sci Part B: Polym Phys 1999, 37, 2069.
16. Utracki, L. A. Polymer Alloys and Blends: Thermodynamics and Rheology, 1st ed.; Hanser: Munich, 1989; Chapter 5.
17. Sai, S.; Mulliken, A. D.; Boyce, M. C. Int J Solids Struct 2007, 44, 2381.
18. Kim, S. J.; Kim, D. K.; Cho, W. J.; Ha, C. S. Polym Eng Sci 2003, 43, 1298.
19. Machado, A. V.; Duin, M. V.; Covas, J. A. J Polym Sci Part A: Polym Chem 2000, 38, 3919.
20. Li, Y.; Xie, X. M.; Guo, B. H. Polymer 2001, 42, 3419.
21. Yin, J.; Zhang, J.; Yao, Y. J Appl Polym Sci 2006, 102, 841.
22. Wu, S. H. Polymer 1985, 26, 1855.
23. Orazio, L. D.; Greco, R.; Mancarella, C.; Martuscelli, E.; Ragosta, G.; Silvestre, C. Polym Eng Sci 1982, 22, 536.
24. Qiu, Z. M.; Wang, J. H.; Zhang, S. B.; Ding, M. X. Polymer 2006, 47, 8444.
25. Tseng, F. P.; Lin, J. J.; Tseng, C. R.; Chang, F. C. Polymer 2001, 42, 713.
26. Liu, Y. Q.; Kontopoulou, M. Polymer 2006, 47, 7731.
27. Matjaz, D.; Vojko, M.; Ivan, S. Compos Part A: Appl Sci Manuf 2005, 36, 1282.
28. Vivek, T.; Richard, L.; Thomas, N. Polymer 2006, 47, 5392.
29. Wong, S. C.; Mai, Y. W. Polymer 2000, 41, 5471.
30. Xie, M. J.; Li, H. L. Eur Polym J 2007, 43, 3480.
31. Yin, Z. H.; Zhang, X. M.; Zhang, Y. J.; Yin, J. H. J Appl Polym Sci 1997, 63, 1857.
32. Bucknall, C. B.; Heather, P.; Lazzeri, A. J Mater Sci 1982, 24, 1489.
33. Yee, A. F.; Li, D.; Li, X. J Mater Sci 1993, 28, 6392.
34. Parker, D. S.; Sue, H.; Huang, J.; Yee, A. F. Polymer 1990, 31, 2267.
35. Kinloch, A. J.; Shaw, S. J.; Hunston, D. L. Polymer 1983, 24, 1341.
36. Margolina, A.; Wu, S. H. Polymer 1988, 29, 2170.
37. Wu, S. H. J Appl Polym Sci 1988, 35, 549.
38. Wu, S. H. Polymer 1990, 31, 971.